Journal Homepage: - www.journalijar.com
INTERNATIONAL JOURNAL OF ADVANCED RESEARCH (IJAR)
Article DOI: 10.21474/IJAR01/3937
DOI URL: http://dx.doi.org/10.21474/IJAR01/3937

RESEARCH ARTICLE

FAULT DIAGNOSIS ON BEARINGS IN SYNCHRONOUS MACHINE BY PROCESSING VIBRO-ACOUSTIC SIGNALS USING HIGHER ORDER SPECTRAL.

Zulma Yadira Medrano Hurtado[1] and Humberto Marcelo[2]

1. Department of Electrical Engineering, Instituto Tecnológico de Mexicali, Mexicali, Baja California, México.
2. Imperial Valley College, Calexico California, U.S.A.

Manuscript Info

Manuscript History

Received: 15 February 2017
Final Accepted: 19 March 2017
Published: April 2017

Key words:-
Higher order spectral, piezoelectric accelerometers, omnidirectional microphones, failure, bearing.

Abstract

This work presents a methodology for detecting faults in synchronous generator bearings using vibration signals recorded by acceleration transducers (piezoelectric accelerometers) and acoustic transducers (omnidirectional microphones). The advantage of using the spectra of higher-order ($HOSA$) in the diagnosis of faults in rotating electric machines bearings is analyzed. A comparison for two special cases of ($HOSA$) was made: spectral density of power (PSD) and biespectrum (BIS). Vibration signals of bearings without fail and with an artificially induced failure were analyzed. The artificial fault consisted of a crack produced on a $SKF6303-2RSH$ bearing cage. This procedure allowed to determine that the BIS shows much more clearly the frequencies generated by the defective bearing.

Introduction:-

Synchronous generators produce about 99% of the electricity consumed all over the world (Medrano et al., 2015a). Because of this great importance in the global electricity generation it is necessary to prevent the occurrence of failures which could possibly cause unwanted problems. Such generators are generally exposed to a large number of faults and are the most expensive equipment of the power system placing them in a critical position Suarez (1998). Failure of bearings is one of the most common problems in synchronous generators, approximately 40% of faults in rotating electrical machines (Sin et al., 2003), (Medrano et al., 2013), (Medrano et al., 2014), (Medrano et al., 2016).

The conventional way of analysis and fault diagnosis of bearings is based on recording vibration signals from accelerometers that play an important role in predictive maintenance of electrical machines. Vibration signals caused by a bearing may contain spectral components that are related to the bearing geometry, the number of rolling elements, the rotation speed, the location of the fault and the type of load applied.

Thus, a window of opportunity of having a different but equally reliable methodology arises by using another type of signal which is not invasive neither expensive. This allows us to propose a diagnosis-system based on the acoustic emission of machines using microphones and sensors. This technique detects internal acoustic changes caused by phenomena such as the emergence and growth of cracks, detachment of small pieces of material, metal deformation, among others, and it is based on that part of the energy released is transmitted outside as sound waves. These acoustic waves can be recorded by means of transducers (microphones) installed in the vicinity of the generator. At the same time, these transducers convert the waves of sound into electrical signals that can then be processed and analyzed for obtaining a diagnosis.

Corresponding Author:- Zulma Yadira Medrano Hurtado.
Address: Department of Electrical Engineering, Instituto Tecnológico de Mexicali, Mexicali, Baja California, México.

The information provided from vibration signals through acceleration or acoustic transducers in the frequency domain can be processed and analyzed to determine possible abnormal conditions in the bearings of synchronous generators. Earlier detection of bearing failures analyzing vibration signals requires the use of appropriate techniques of signal processing that involves higher-order spectra analysis ($HOSA$).

Causes of bearing failure:-

Among the most commonly identified causes of failure on bearings are: adequate lubrication, 36%; improper operation (excessive dynamic loads on the bearing, imbalance and misalignment), 34%; contamination (including moisture), 14%; and about 16% due to defects from other factors such as transportation/storage problems or inadequate bearing installation (Medrano et al. 2016). In most cases, failures do not appear suddenly bu gradually making possible their detection before a catastrophe occurs.

Vibration Analysis:-

Under normal operating conditions, bearings would fail due to wear or fatigue of the material, and when such a failure appears vibrations and acoustic emission levels in a synchronous generator increase too. These bearings fault frequencies are a function of geometry of the bearings and driving speed (Stack et al., 2004), Palomino (2011), Wowk (1991). Each one of the components of a bearing has a particular fault frequency that might be identified depending on the element failed and it should be defined by at least one of four characteristic frequencies when occurring in: the outer race ($BPFO$, ball pass frequency of the outer race), the inside track ($BPFO$, ball pass frequency of the inner race), the rolling elements (BSF, ball spin frequency), the cage (FTF, fundamental train of frequency).

$$BPFO = \frac{ne}{2} \cdot \frac{V_{rpm}}{60} \cdot \left[1 - \frac{d}{D} \cdot cos(\beta)\right] \quad (1)$$

$$BPFI = \frac{ne}{2} \cdot \frac{V_{rpm}}{60} \cdot \left[1 + \frac{d}{D} \cdot cos(\beta)\right] \quad (2)$$

$$BSF = \frac{D}{d} \cdot \frac{V_{rpm}}{60} \cdot \left[1 - \left(\frac{d}{D}\right)^2 \cdot cos^2(\beta)\right] \quad (3)$$

$$FTF = \frac{V_{rpm}}{120} \cdot \left[1 - \frac{d}{D} \cdot cos(\beta)\right] \quad (4)$$

where D is the pitch diameter (mm), d is the diameter of balls (mm), β is the contact angle between the balls and tracks (°), V_{rpm} is the rotation speed (rpm), and ne is the number of rolling elements.

Failure frequencies are reference points when analyzing the spectrum obtained from the vibration signals of bearing, because if there is a problem, the spectrum provides information to determine the location, the cause, and how critical the problem could it be Suarez (1998).

Theoretical framework:-

If analyze an infinite-length signal composed of a sinusoid

$x(t) = Asin(\omega t + \theta), -\infty < t < +\infty$ (5)

were: A is the amplitude; ω is the frequency in $^{rad}/_{sec}$; θ is the phase angle in rad

When taking part of the signal $x(t)$, with a length of N whole samples comprised in the interval $0 \leq n \leq N-1$, allows to define a new signal that is denoted as $x(n)$. This signal can be thought of as the result of multiplying the original signal $x(t)$ by a window $w[n]$.

$x(n) = x(t)w[n]$ (6)

Second-order statistics (PSD):-

PSD is currently the most used tool for analyzing frequency signals. If $x(t)$ is a stochastic signal with zero mean, the PSD is defined as (Nikias et al., 1987), (Proakis et al., 1998), (Ypma et al., 1997):

$PSD_x(\omega) = \int_{-\infty}^{+\infty} x(n)e^{\{-j(\omega n)\}}d\omega$ (7)

where $\omega = 2\pi f$

The second-order cumulant is defined as:

$$C_{2x} = E[x(t)\, x(t+\tau_1)] \quad (8)$$

where $E[\ ]$ is the mathematical expectation operator in random variables, either of a data set or a function related with the data between the square brackets. The PSD can then be rewritten as:

$$PSD_x(\omega) = \int_{-\infty}^{+\infty} c_{2x}(\tau) e^{\{-j(\omega\tau)\}}\, d\tau \quad (9)$$

where τ is the time delay variable, ω is the frequency variable.

$$PSD_x(\omega) = \int_{-\infty}^{+\infty} x^2(t)\, d\tau = \int_{-\infty}^{+\infty} P_x(\omega)\, d\omega \quad (10)$$

The frequency spectrum can be represented as:

$$PSD_x(\omega) = X(\omega)X^*(\omega) = |X(\omega)|^2 \quad (11)$$

where $X(\omega)$ is the Fourier transform signal, $X^*(\omega)$ is the conjugate of the function, and $|X(\omega)|$ is the amplitude function. The power density method has limitations such as loss of signal phase, inability to detect non-stationary signals, and cannot be detected when two signal frequencies are equal or very similar that could be overlapped. Because of this some limitations could result in detecting and diagnose a failure in the machine.

Statistics of third order ($HOSA$):-

The *BIS* is a particular case of higher-order spectra and by definition is a two-dimensional Fourier transform of the third order cumulants (Gomez and Paredes, 2005), (Toledo et al., 2001), (Nikias and Mendel, 1990), Rivola (2000), (McCormick and Nandi, 1999), Mendel (1991), (Swami et al., 1998), (Brillinger and Murray, 1967). One of the main reasons for the use of BIS is that provides information about the amplitude and phase of the signals.

If $x(t)$ is a stochastic signal with zero mean, the *BIS* is defined as:

$$BIS_x(\omega_1, \omega_2) = \int_{-\infty}^{+\infty} x(t)x(t+\tau_1)x(t+\tau_2) e^{\{-j(\omega_1\tau_1+\omega_2\tau_2)\}} d\tau_1 d\tau_2 \quad (12)$$

It can be seen that the bispectrum is a function of two independent variable frequencies (ω_1 and ω_2). The BIS reflects the interaction between ω_1, ω_2 and $\omega_1 + \omega_2$.

The third-order cumulant is defined as:

$$C_{3x} = E[x(t)\, x(t+\tau_1)x(t+\tau_2)] \quad (13)$$

The BIS can then be rewritten as:

$$BIS_x(\omega_1, \omega_2) = \int_{-\infty}^{+\infty} c_{3x}(\tau_1, \tau_2) e^{\{-j(\omega_1\tau_1+\omega_2\tau_2)\}} d\tau_1 d\tau_2 \quad (14)$$

Similar to PSD, the *BIS* satisfies the following relationship:

$$BIS_x(\omega_1, \omega_2) = \gamma X(\omega_1)\, X(\omega_2) X^*(\omega_1 + \omega_2) \quad (15)$$

where γ is a constant of proportionality, the scale is:

$$BIS(\omega_1, \omega_2) = |BIS(\omega_1, \omega_2)| \quad (16)$$

and the phase is:

$$\varphi(\omega_1, \omega_2) = \phi(\omega_1) + \phi(\omega_2) - \phi(\omega_1 + \omega_2) \quad (17)$$

This result indicates that the BIS has magnitude and phase, which does not happen with the PSD. The BIS has the advantage that being a three-dimensional representation, frequencies can be displayed graphically and making possible to detect coupling between similar frequencies.

Experimental Methodology:-

Figure 1 shows the steps followed for detecting faults in bearings based on vibration analysis (continuous frames), and the steps followed to evaluate the BIS with acoustic transducers (dotted boxes).

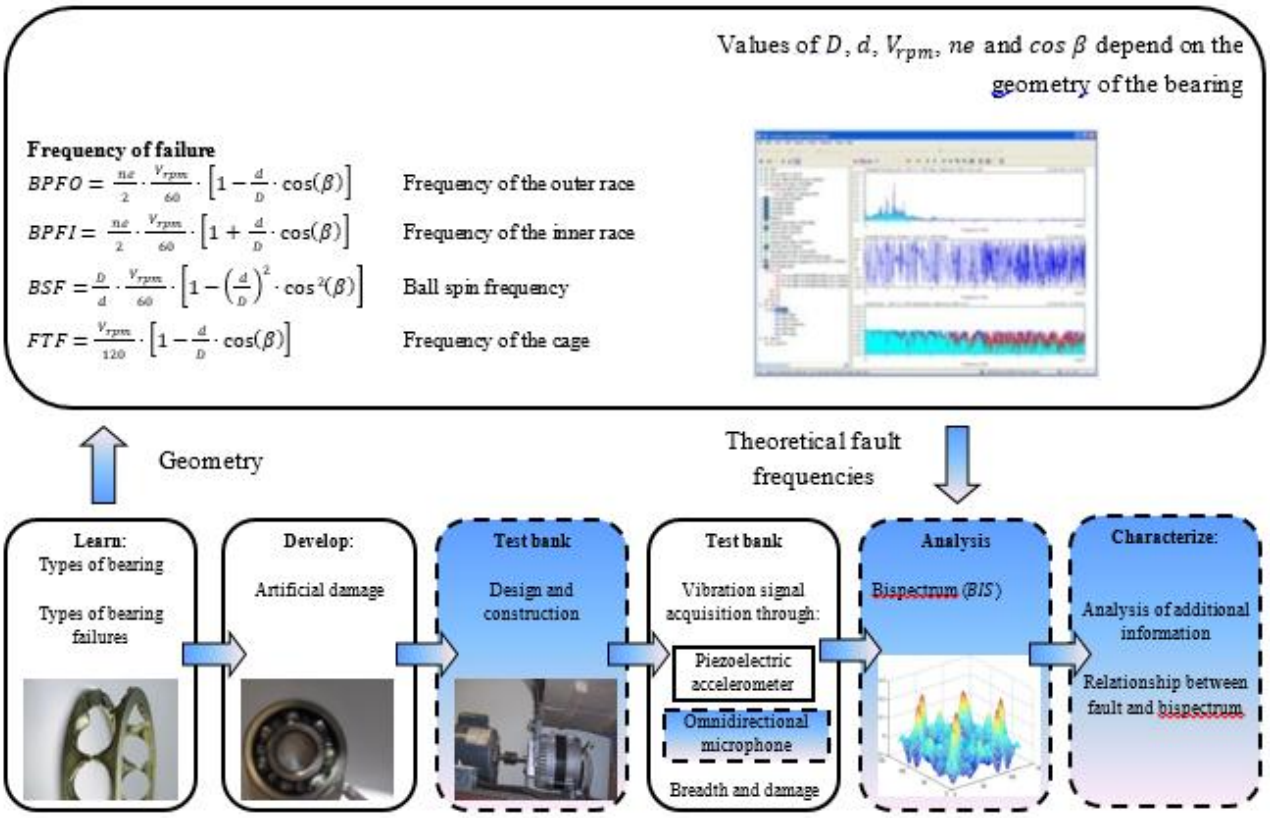

Figure 1:- Methodology of experimentation [19].

Tests and Results:-

First of all, experimental tests were performed in a non-failed new machine and data were collected. After that, a crack was induced in the cage of a bearing $SKF6303-2RSH$. Tests were carried out in a test lab as shown in figure 2 (a), the characteristics of the engine generator system are: GE single phase induction motor, CATNO. C1158, 1hp, 60Hz, $115/208-230$ V, 1725 rpm, 14.7 A, synchronous generator 2 hp, 50 Vcd. Acceleration transducers (piezoelectric accelerometers, Analog Device ADXL325 – EVAL) and acoustic transducers (omnidirectional microphones, Panasonic WM – 55A103) were used for vibration analysis.

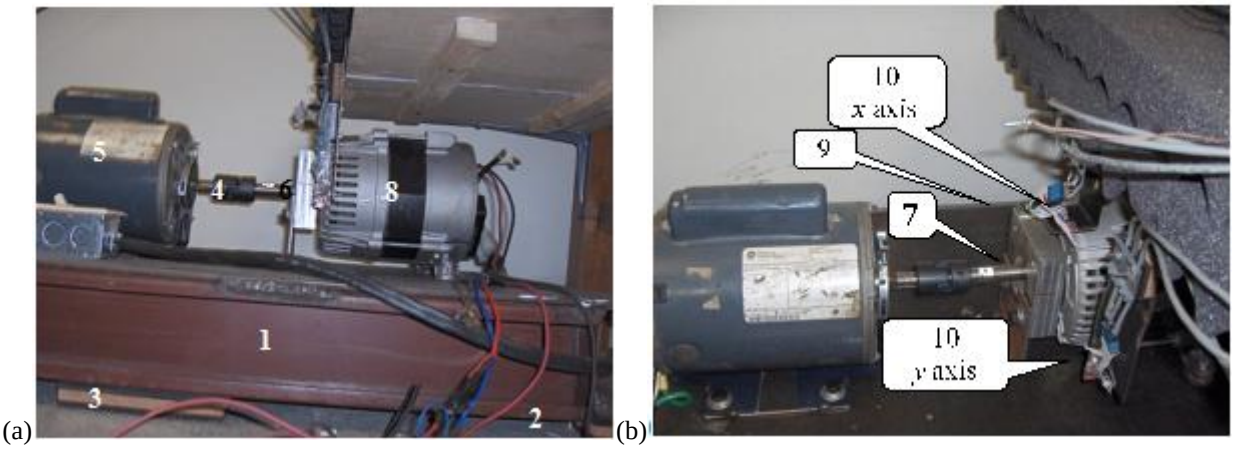

Figure 2:- Mechanical system: (a) experimental arrangement, (b) location of the transducers.

Table 1:- Features of the test bank.

Num.	Qty	Description
1	1	Metalic base ($6.35x10^{-3}\ m$)
2	4	Cork and neoprene vibration dampers
3	4	Screws
4	1	Lovejoy coupling $12.7x10^{-3}$ at $12.7x10^{-3}\ m$
5	1	Single phase induction motor $GE, CATNO.C\ 1158, 1\ Hp,\ 60\ Hz, \frac{115}{208} - 230\ V,\ 1725\ rpm,$ $14.7\ A.$
6	1	Aluminum base ($0.1x0.1x0.03\ m$)
7	2	$SKF6303 - 2RSH$ Bearing
8	1	Synchronous generator, $2Hp$, $50\ Vdc$
9	1	3-axes accelerometer (Analog Device $EVAL -$ ADXL325)
10	2	Omnidirectional microphone (Panasonic WM $-$ 61A)

Bearing failure frequencies $SKF6303 - 2RSH$:-

When deterioration occurs on a single component of the bearing then a peak at a particular frequency appears and its value depends on the geometry of the bearing and its rotation speed. Palomino (2011), (SKF. Frequency calculator-Bearing frequencies calculation) Bearing characteristics for calculating the frequencies of vibration of the equations 1 to 4 are (SKF. Frequency calculator-Bearing frequencies calculation): $D = 32\ mm,\ \ d = 8.731mm,\ \ \beta = 0°,$ $ne = 7\ balls,\ \ V_{rpm} = 1725\ rpm$. In Table 2, the values of the vibration frequencies for the bearing elements are listed.

Table 2:- Frequency of failure for the bearing elements $SKF6303 - 2RSH$.

Rotational frequencies		Frequencies (*Hz*)				
Hz	*rpm*	Inner race defective Hz ($BPFI$)	Outer race defective Hz ($BPFO$)	Cage defective Hz (FTF)	Frequency of ball rotation Hz (BSF)	Defects in balls Hz
60	1725	128.080	73.170	10.453	48.764	97.527

Vibration and acoustic bearing signals were acquired by means of a data acquisition-card $NI\ USB - 6009$, taking a representative sample of 6000 points recording the sample after five minutes operation once the machine was running stable.

Analysis of the signal in the frequency domain PSD (accelerometers and microphones):-

Figures 3 and 4 show the results obtained for the horizontal signal (x axis) and vertical (y axis) of the generator piezoelectric accelerometer. In each case, the signals are plotted as amplitude vs. frequency for (a) *without* failure and (b) *with* failure (crack in the bearing).

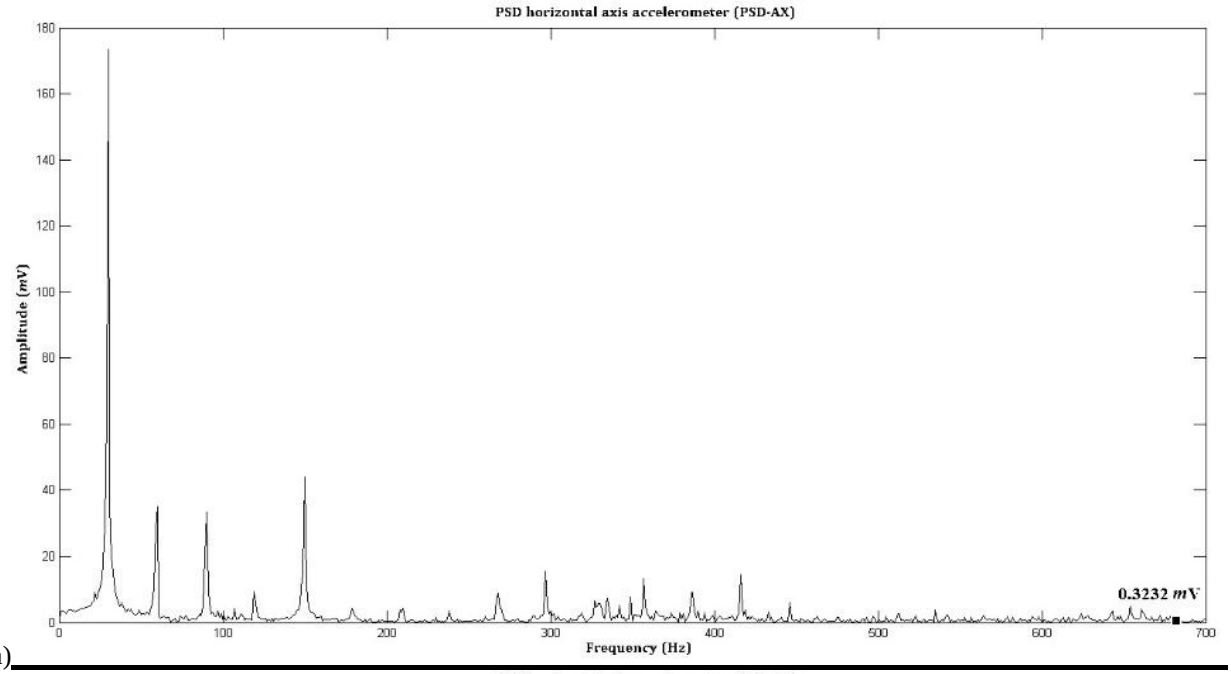

(a)

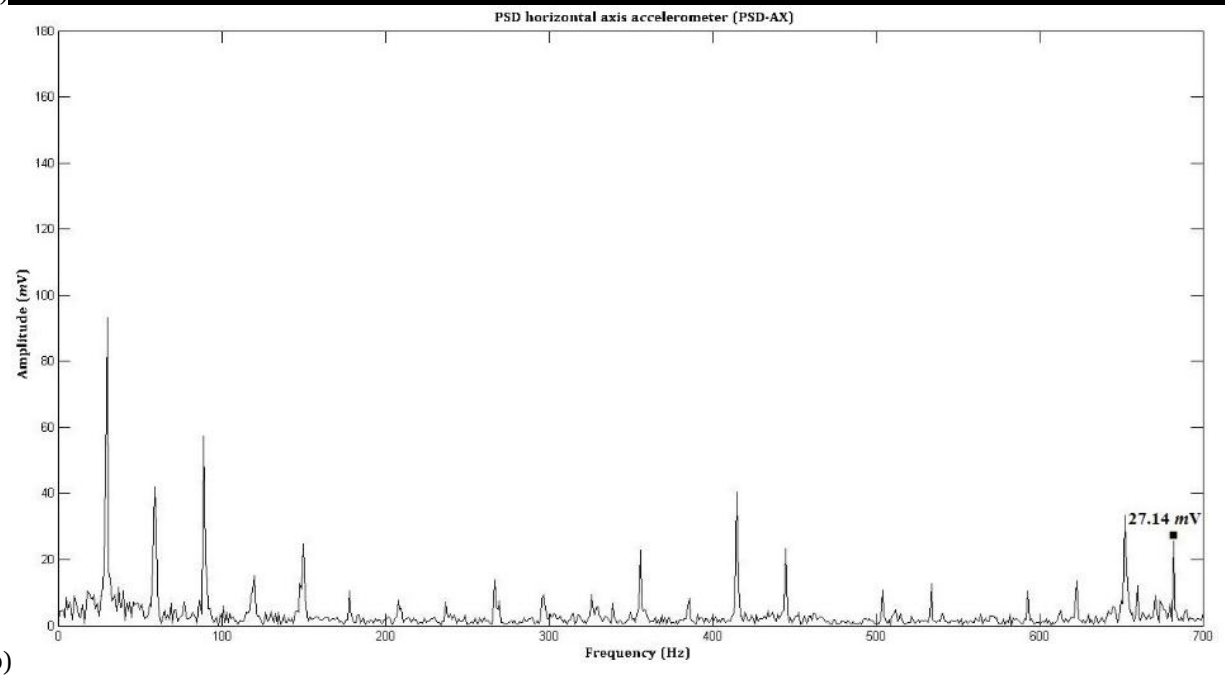

(b)

Figure 3:-Vibration signal of the piezoelectric accelerometer with respect to x axis for: (a) *without* failure, (b) *with* failure.

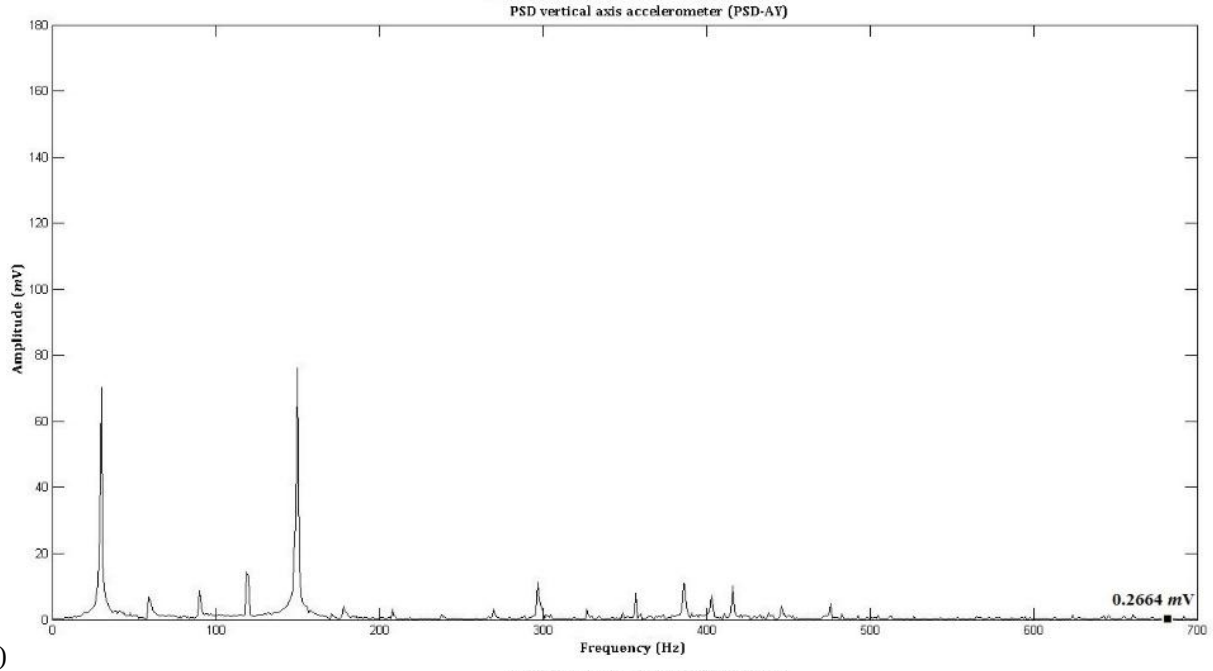

(a)

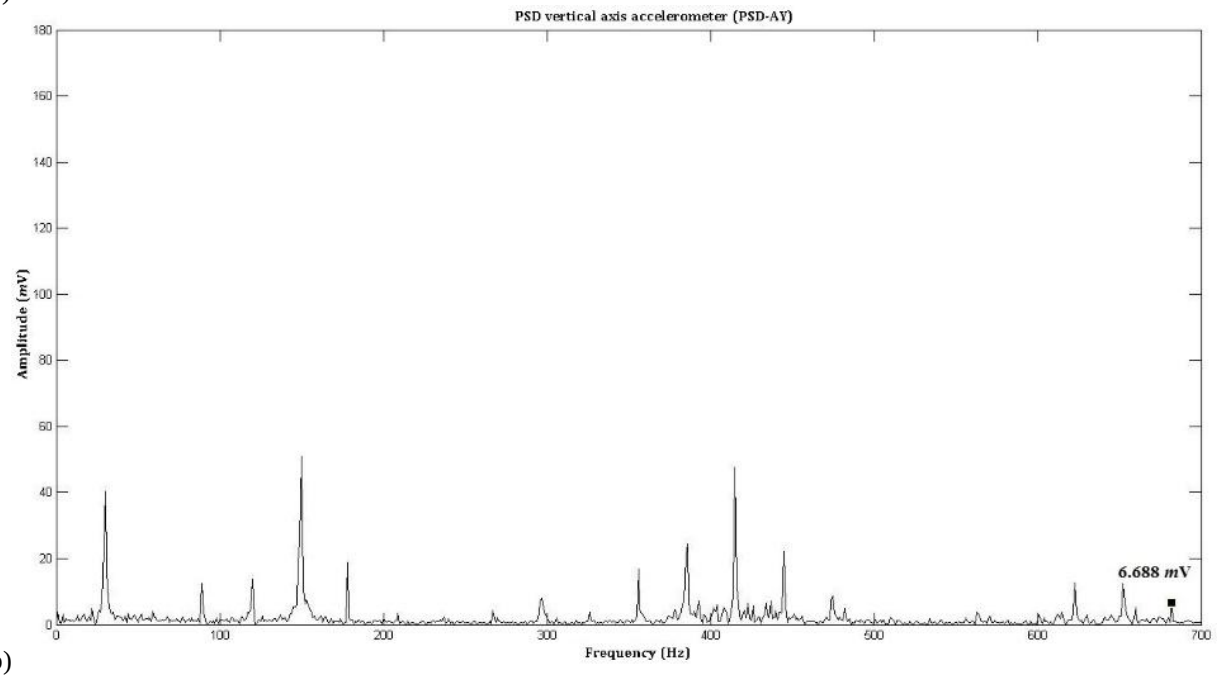

(b)

Figure 4:- Vibration signal of the piezoelectric accelerometer with respect to *y* axis for: (a) *without* failure, (b) *with* failure.

Similarly, when an omnidirectional microphone is used the amplitude vs. frequency for the x and y axis, the acoustic signals recorded are shown in figures 5 and 6.

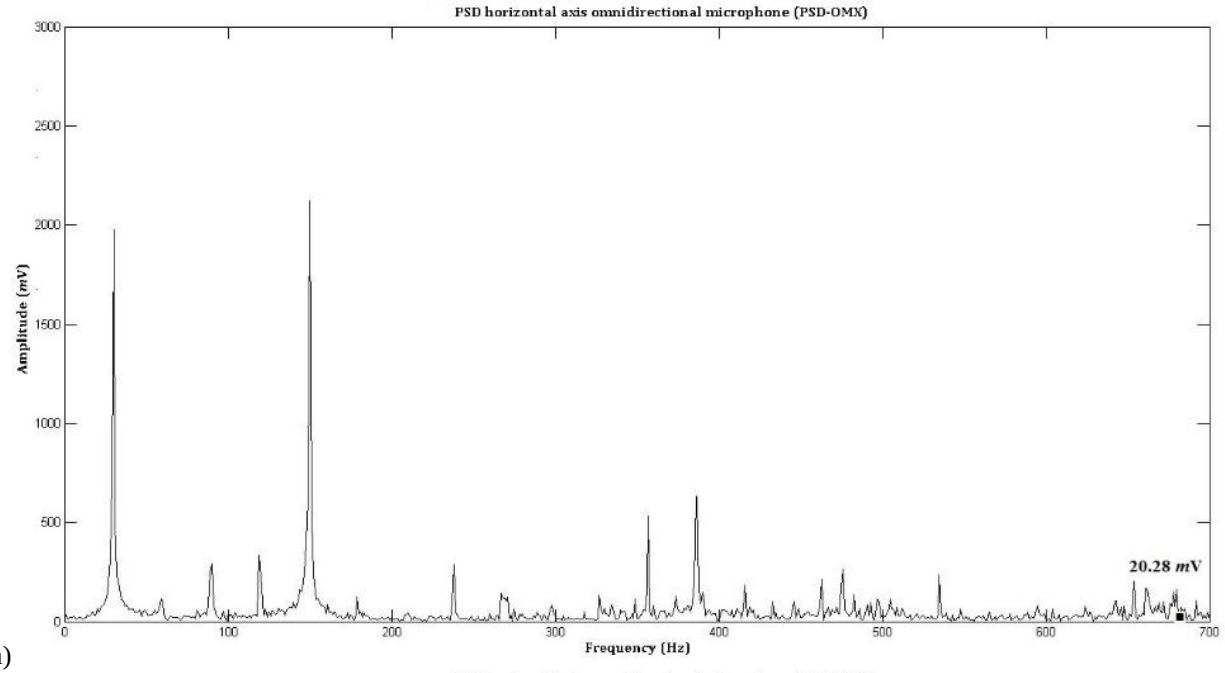

(a)

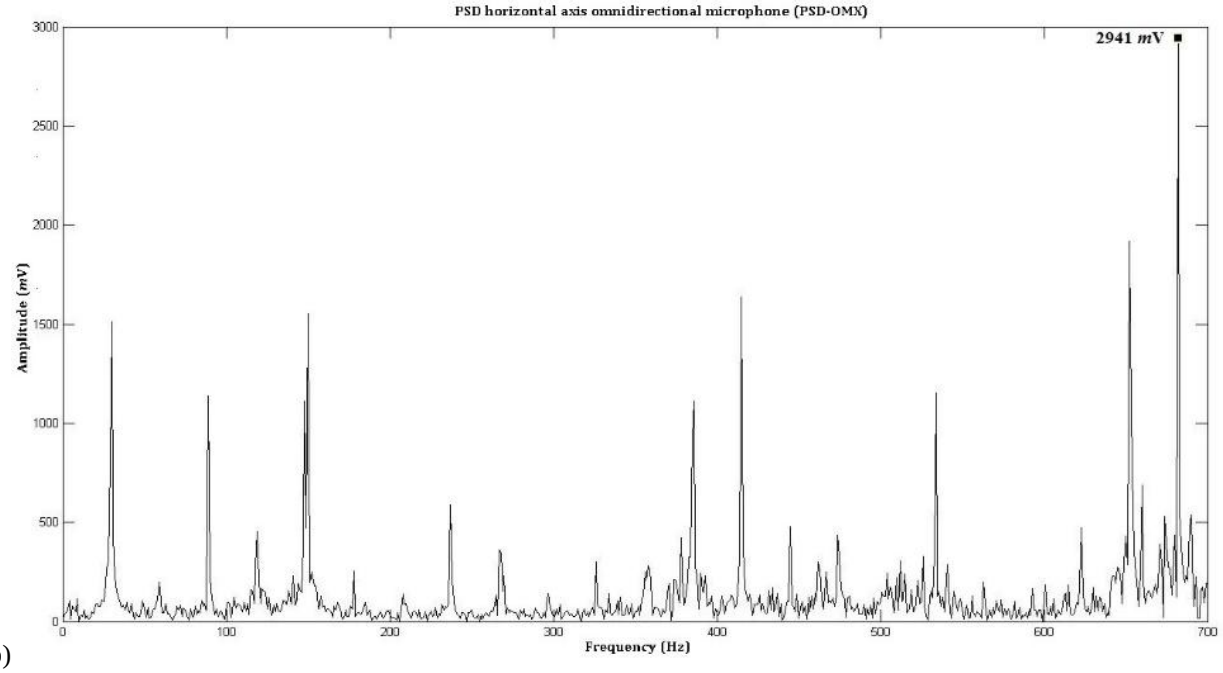

(b)

Figure 5:- Acoustic signal from omnidirectional microphone with respect to x axis for: (a) *without* failure, (b) *with* failure.

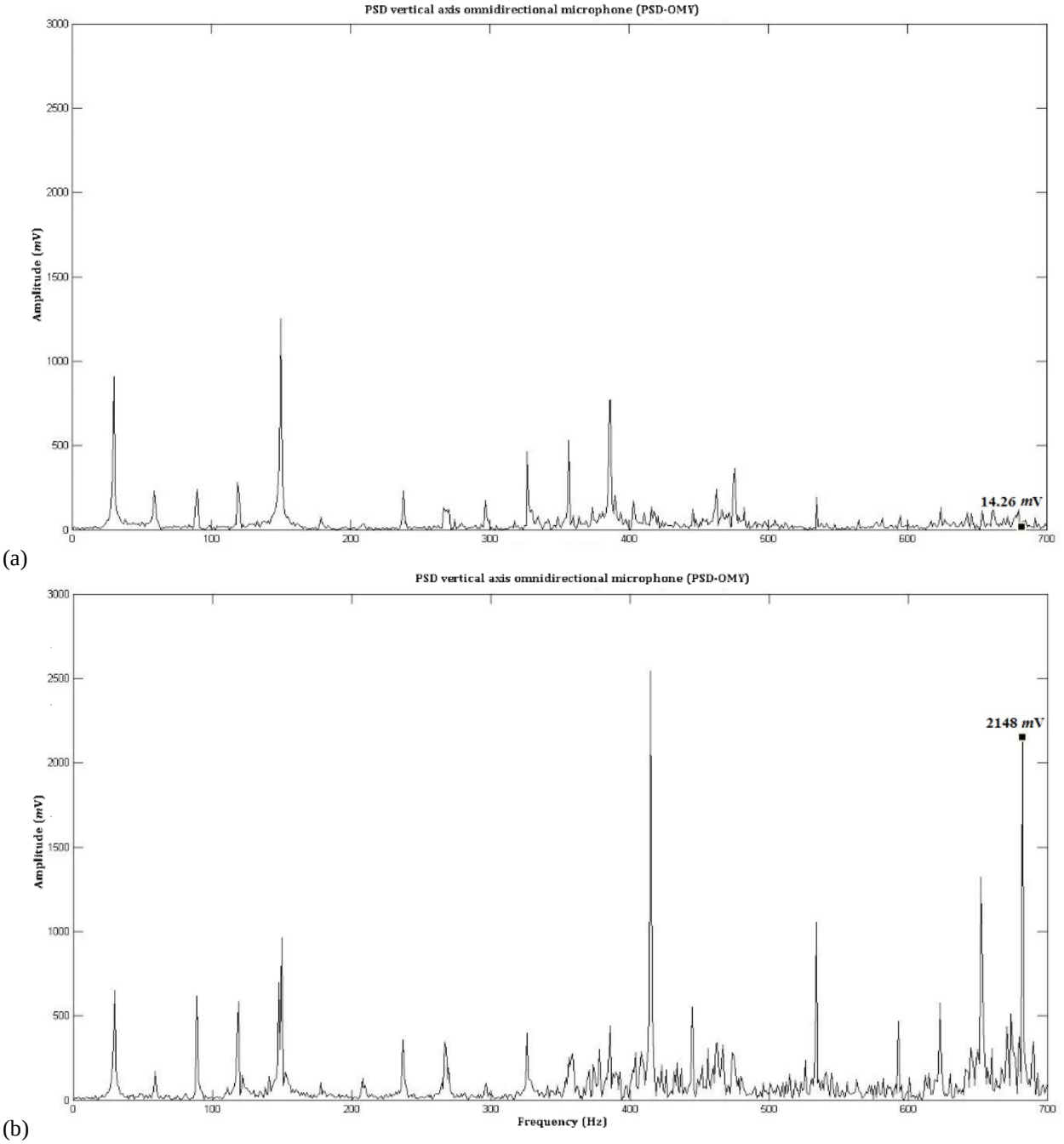

Figure 6:- Acoustic signal from omnidirectional microphone with respect to *y* axis for: (a) *without* failure, (b) *with* failure.

The effect of signal overlapping when *PSD* analysis is used is quite explained in (Ypma et al., 1997). In this work the analysis was performed for a frequency of 682 Hz which is about 23 times the frequency of rotation of the shaft.

In figure 3 (a), with the accelerometer, the vibration signal amplitude of the x component *without* failure is 0.3232 mV / Hz and while *with* failure is 27.14 mV/Hz (figure 3 (b)). In figure 4 (a) the amplitude of the y component without failure is 0.2664 mV/Hz while with failure is 6688 mV/Hz (figure 4 (b)).

For the microphone, the acoustic signal amplitude of the x component *without* failure is 20.28 mV/Hz whilst *with* failure is 2941 mV/Hz (figure 5(a) and (b)). For y axis the-amplitude *without* failure was 14.26 mV/Hz whilst *with* failure was 2148 mV/Hz (figure 6 (a) and (b)).

When the fault is severe there appear sidebands around the important frequencies of rotation of the machine. In figures 3, 4, 5 and 6, frequency peaks of 30, 60, 89 and 119 Hz were analyzed. It was observed that these frequencies are closely related as multiples of 30 Hz which is the theoretical frequency of shaft rotation.

Analysis of the signal *BIS* (accelerometers and microphones):-

Figures 7 and 8 show the results obtained for the signal in the x and y axis from piezoelectric accelerometers. In each case, the signals are plotted in amplitude of the *BIS* for (a) *without* failure and (b) *with* failure (crack in the bearing).

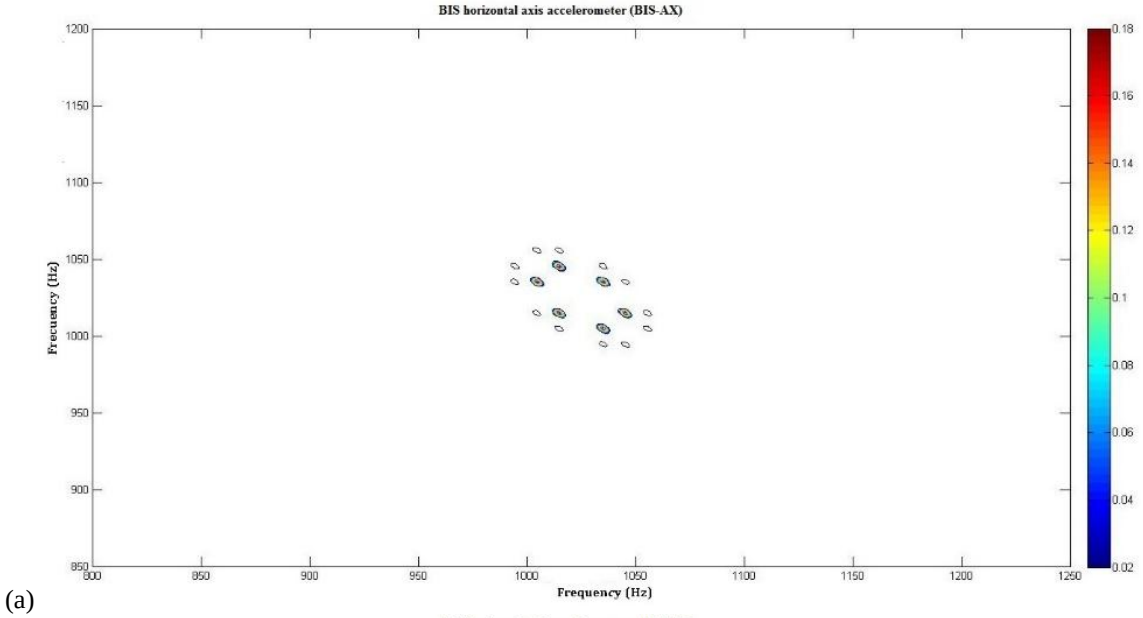

(a)

(b)

Figure 7:- Vibration signal of the piezoelectric accelerometer with respect to x axis for: (a) *without* failure, (b) *with* failure.

(a)

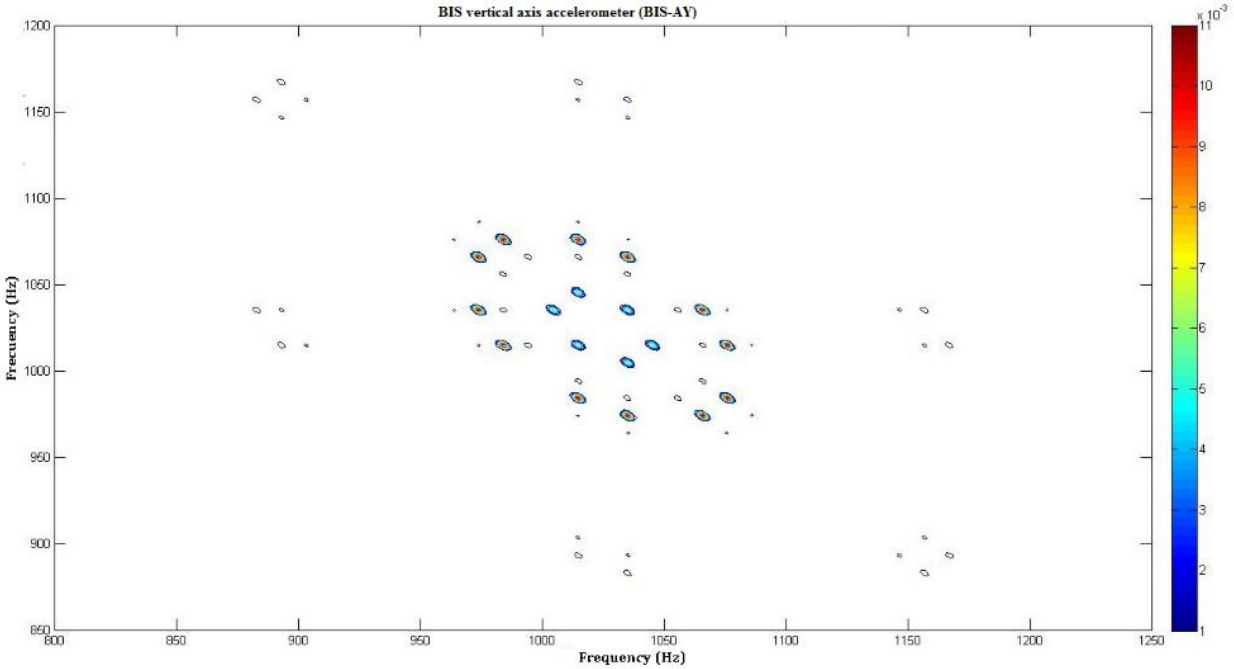

(b)

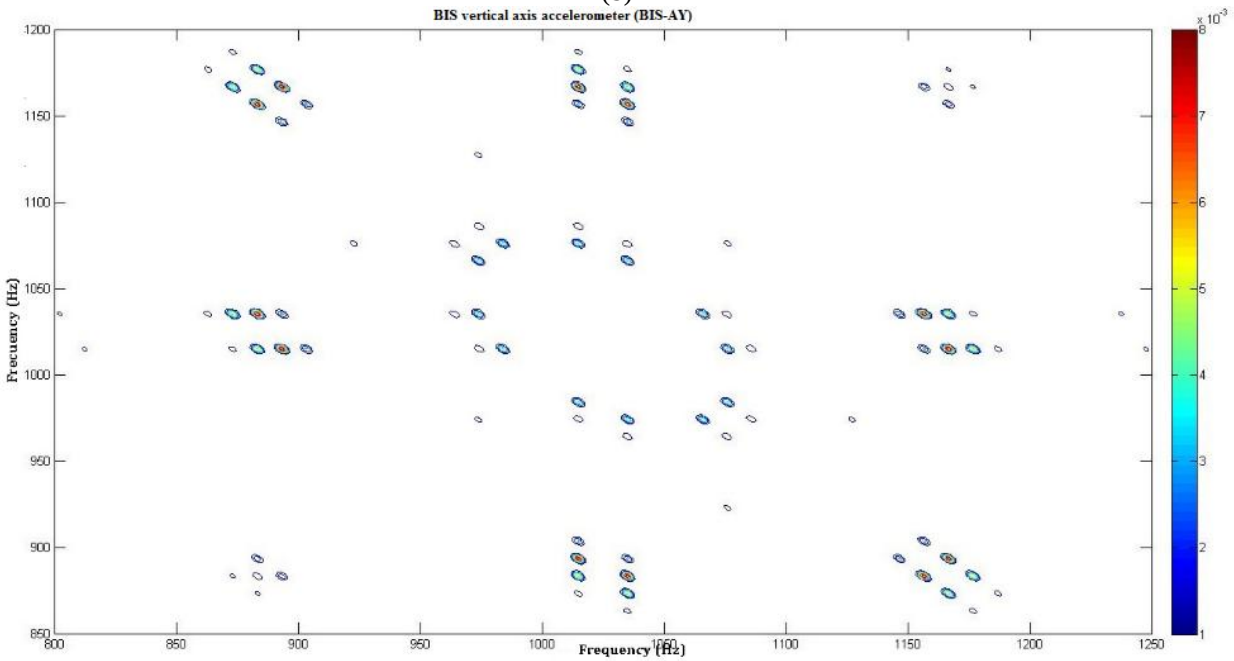

Figure 8:- Vibration signal of the piezoelectric accelerometer with respect to *y* axis for: (a) *without* failure, (b) *with* failure.

Similarly, for the case where omnidirectional microphone was used the acoustic signals components in the x and y axis for the bearing *without* failure and *with* failure are shown in figures 9 and 10.

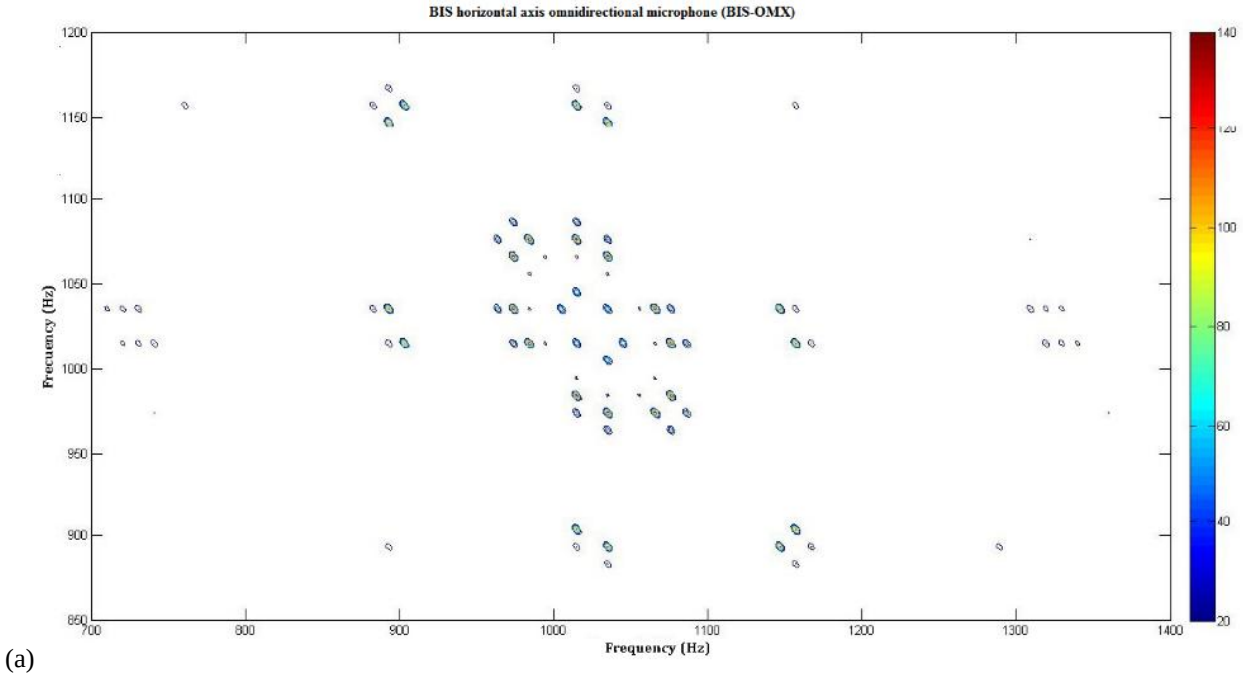

(a)

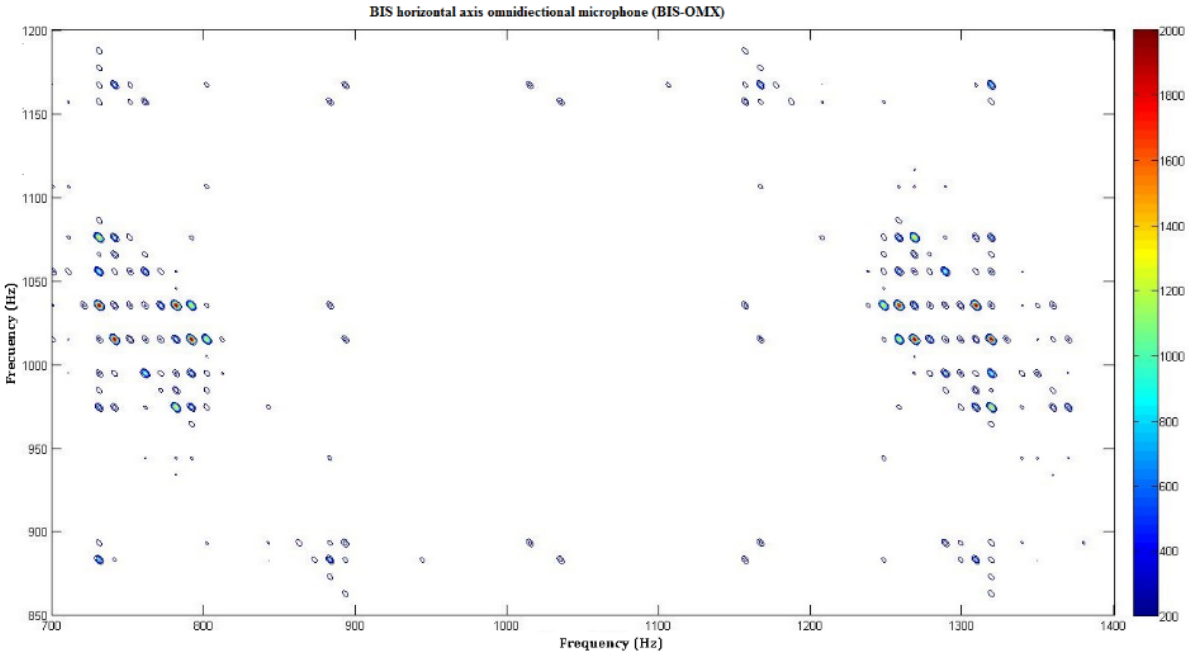

(b)

Figure 9:- Acoustic signal of the omnidirectional microphone with respect to x axis for: (a) *without* failure, (b) *with* failure.

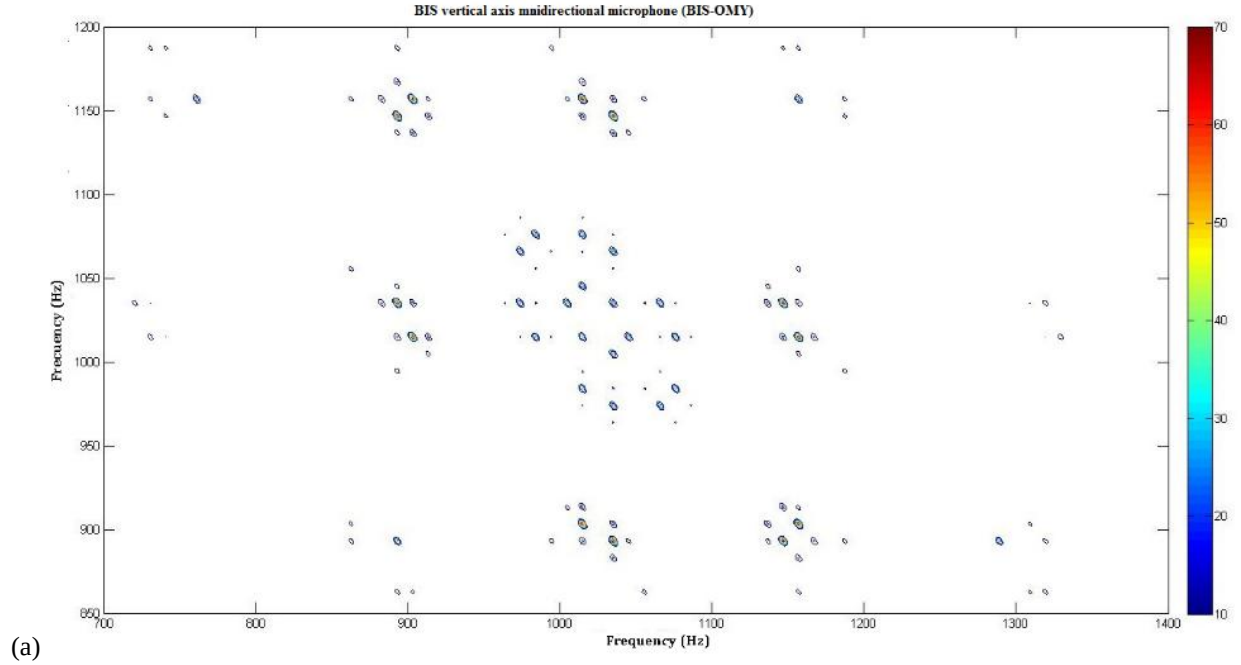

(a)

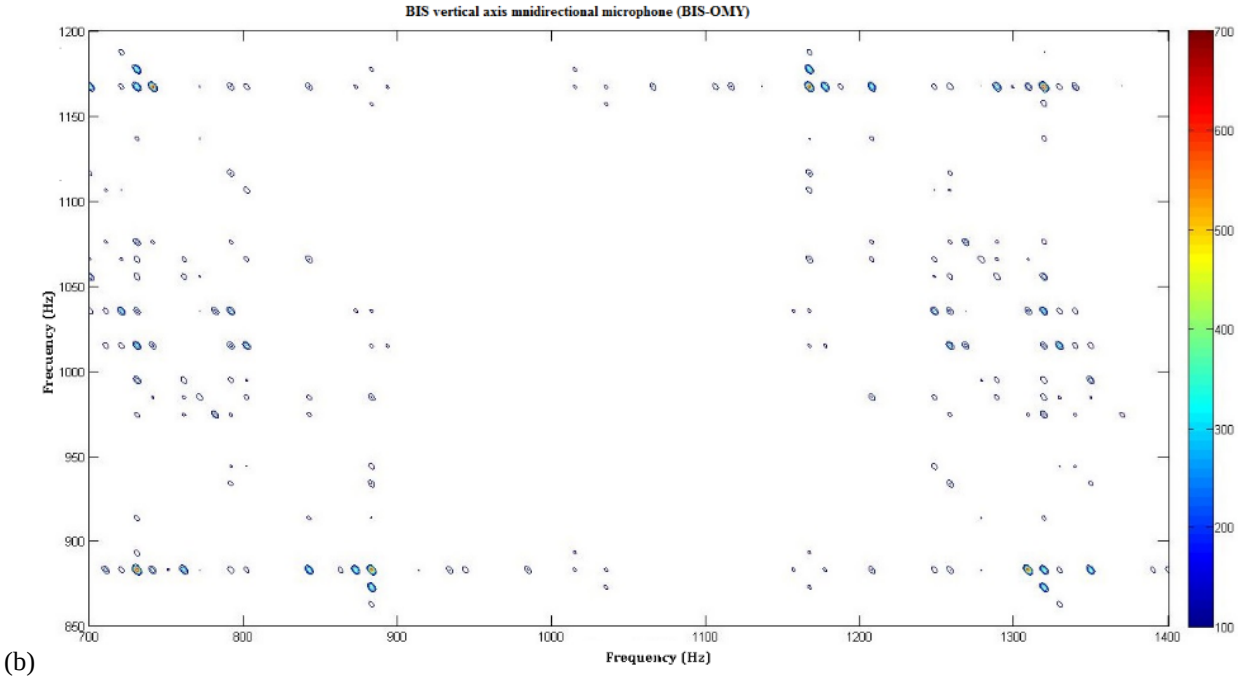

(b)

Figure 10:- Acoustic signal of the omnidirectional microphone with respect to *y* axis for: (a) *without* failure, (b) *with* failure.

In figures 7 and 8, when an accelerometer was used for both x and y axes the components of the vibration signal *without* failure and *with* failure exhibit couplings at 30 Hz that represents the theoretical frequency of shaft rotation.

In figures 9 and 10, from the microphone signals, on both the x and y axes it is observed acoustic couplings *without* failure signal frequency 30 Hz it represents the theoretical frequency of shaft rotation. And with failure has coupling to 11 Hz frequency representing the frequency of failure of the bearing cage.

When the fault is in the bearing cage the frequencies of failure, decrease or disappear due to the occurrence of many components at random frequencies that prevent the formation of sidebands around the frequency of failure,

presenting an increase in background noise (Medrano et al. 2015b). This prevents to make a diagnosis for failure in the bearing cage through the use of accelerometers, but allows the use of microphones in detecting these.

Discussion and Analysis:-

Results of graphic signals with respect to the frequency (PSD):-

a. Frequency peaks that occur in the $PSD's$ of the accelerometer signals in the x and y axes for the condition without failure are related to the theoretical frequency of shaft rotation (approximately 30 Hz).
b. The peaks that occur in the $PSD's$ of the accelerometer signals in the x and y axes for the condition with failure are related to the theoretical frequency of shaft rotation (approximately 30 Hz), the theoretical frequency of failure for the bearing cage (approximately 11 Hz) is masked by other frequencies of operation of the machine which makes it complicated to make a diagnostic resolution with this type of graph.
c. The peaks that occur in the $PSD's$ of acoustic signals in the x and y axes for the condition *without* failure, is less regarding the condition *with* failure, the frequency peaks related to the theoretical frequency of shaft rotation (approximately 30 Hz).
d. The peaks that occur in the $PSD's$ of acoustic signals in the x and y axes for the condition *with* failure is related to the theoretical frequency of shaft rotation (approximately 30 Hz), the theoretical frequency of failure for the bearing cage (approximately 11 Hz) is masked by other frequencies of operation of the machine which makes it complicated to make a diagnostic resolution with this type of graph.

Results of graphic signals bispectrum (BIS):-

a. The couplings presented in the BIS accelerometer signals in the x and y axes for the condition *without* failure are related to the theoretical frequency of shaft rotation (approximately 30 Hz).
b. The couplings presented in the BIS accelerometer signals in the x and y axes for the faulted condition is related to the theoretical frequency of shaft rotation (approximately 30 Hz) couplings caused by the defect frequency (approximately 11 Hz) is attenuated or not displayed due to the appearance of many components of random frequencies, making it difficult to identify couplings caused by the defect often as many couplings are of small amplitude and are masked by other frequencies of operation of the machine making it complicated to make a diagnostic resolution with this type of graph.
c. Couplings often presented in the BIS of acoustic signals in the x and y axes for *without* failure condition are lower with respect to the condition with failure. Appearing frequency peaks related to the theoretical frequency of shaft rotation (approximately 30 Hz).
d. The couplings presented in the BIS of acoustic signals in the x and y axes for the condition *with* failure are related to the theoretical frequency of failure for the bearing cage (approximately 11 Hz) is present in a clear and obvious way.
e. With $BIS's$ obtained in both axes (for faulty condition) spaced by the frequency of failure for the bearing cage $SKF6303 - 2RSH$ peaks are observed. So the BIS obtained through acoustic signals in horizontal axis (x) and vertical (y) allows this type of methodology is appropriate for the detection of this type of bearing failure.

Conclusions:-

An acquisition system which consisted of triaxial piezoelectric accelerometers, omnidirectional microphones in the x and y axes are used for the experimental phase. An analysis of the results it can be deduced that:

1. Piezoelectric accelerometers detect no significant differences for conditions without failure and failure so it is concluded that this type of transducers are not a viable alternative for fault detection analysis of vibration signals.
2. Omnidirectional microphones are capable of detecting a fault in the bearing cage of a synchronous generator in both the x direction and in the direction and from the acoustic signals emitted by it.
3. The increased width of the sound level is a parameter that allowed detect bearing damage, while the number of separated peaks failure frequency allowed to determine the location of damage in the cage.

Leading to the conclusion that the use of omnidirectional microphones is a viable option for the detection of bearing failures in a synchronous generator, performing the analysis of the signals through the BIS, which allows monitoring the evolution of the spectrum signals which can be detected any abnormal signs or changes that could indicate a possible failure ahead.

Scientific innovation:-

A methodology that uses signal processing technique for analyzing *BIS* acoustic signals of synchronous generators, which can identify early failures in their bearings and establish accurate and reliable diagnosis less invasive than those obtained by the methods used so far.

Biography:-

Zulma Yadira Medrano-Hurtado. Engineer electrician, Professor of the Institute Institute of Technology of Mexicali (ITM), in Mexicali Baja California Mexico. She earned the master's degree in electrical engineering in the area of metrology and Instrumentation (2007). She obtained a doctorate in electrical engineering in the area of metrology and Instrumentation (2014) by the Institute of engineering of the Autonomous University of Baja California (UABC). Here areas of interest: Metrology and instrumentation, data acquisition, signal processing analysis and diagnostics of electrical machines. She has published several articles in academic journals in 2013 in the Nueva Granada magazine "Un Estudio sobre la Localización, Detección y Diagnóstico de Fallas en Máquinas Eléctricas", in 2014 in magazine publications in science and technology. Universidad Centroccidental Lisandro Alvarado "A review on detection and fault diagnosis in induction machines". in 2015 in Journal of Engineering Science and Technology Review "A Review on Detection and Fault Diagnosis in Induction Machines", in 2016 in the journal engineering research and technology "Nueva metodología de diagnóstico de fallas en rodamientos en una máquina síncrona mediante el procesamiento de señales vibro-acústicas empleando análisis de densidad de potencia". In 2017 in the Nueva Granada magazine "Validación de señales vibro-acústicas para el diagnóstico de fallas en rodamientos en un generador síncrono".

References:-

1. Zulma Medrano, Carlos Pérez, Julio Gómez. (2015)a. A Review on Detection and Fault Diagnosis in Induction Machines. Journal of Engineering Science and Technology Review. pp.185-195.
2. Alejandro Suarez. (1998). IDEAR. Análisis de Fallas en Rodamientos. pp. 1-20.
3. M. Sin, Wen Soong, Nesimi Ertugrul. (2003). Induction Machine On-line Condition Monitoring and Fault Diagnosis-A Survey. University of Adelaide. pp. 1-6.
4. Zulma Medrano, Carlos Pérez, Marco Armas, Cesar Amaro. (2013). Un Estudio sobre la Localización, Detección y Diagnóstico de Fallas en Máquinas Eléctricas. Universidad Militar Neogranadina. pp. 37-59.
5. Zulma Medrano, Carlos Pérez; Julio Gómez, (2014). A review on detection and fault diagnosis in induction machines. Publicaciones en Ciencias y Tecnología. Universidad Centroccidental Lisandro Alvarado. pp. 11-30.
6. Zulma Medrano, Carlos Pérez, Julio Gómez, Maximiliano Vera. (2016). Nueva metodología de diagnóstico de fallas en rodamientos en una máquina síncrona mediante el procesamiento de señales vibro-acústicas empleando análisis de densidad de potencia. Ingeniería Investigación y Tecnología, volume XVII (number 1). pp 73-85.
7. Jason Stack, Ronald Harley, Thomas Habetler. (2004). An Amplitude Modulation Detector for Fault Diagnosis in Rolling Element Bearing. IEEE Transactions on Industrial Electronics. Vol. 51. pp. 1097-1102.
8. Palomino Evelio. (2011). Elementos de medición y análisis de vibraciones mecánica en máquinas rotatorias. Centro de Estudios Ingeniería de Mantenimiento. Published by: ucv vibraciones mecanicas.
9. Wowk Victor. (1991). Machinery Vibration-Measurement and Analysis. McGraw Hill.
10. Nikias C. L., Raghuveer M. R. (1987). Bispectrum Estimation: A Digital Signal Processing Framework. Proceedings of the IEEE. Vol. 75. No.7. pp. 869-891.
11. Proakis, J.G. & Manolakis D. G. (1998). Tratamiento Digital de Señales. 3ª ed. Prentice-Hall.
12. Ypma Alexander, Upma Er, Ligteringen Ronald, Frietman-Eduard E.E., Duin-Rbert P.W. (1997). Recognition of Bearing Failures using Wavelets and Neural Networks. Pp.1-4.
13. Vicente Gómez, y R. Paredes. (2005). Diagnóstico de Condiciones de Operación de Rodamientos en Máquinas Usando Espectros de Orden Superior. [Master Thesis]. Cuernavaca, México. cenidet.

14. E. Toledo, I. Pinhas, D. Aravot, S. Akselrod. (2001). Bispectrum and Bicoherence for the Investigation of Very High Frecuency Peaks in Heart Rate Variability. Proceedings of the IEEE. Computers in Cardiology. No. 28. pp. 667-670.
15. Crysostomos Nikias, Jerry Mendel. (1990). Introduction Special Section on Higher Order Spectral Analysis. IEEE Trans. On Acoustics, Speech and Signal Processing, Vol. 38.
16. Alessandro Rivola. (2000). Applications Of Higher Order Spectra To The Machine Condition Monitoring. Dipartimento di Ingegneria delle Costruzioni Meccaniche, Nucleari, Auronautiche e di Metallurgia. Pubbl. DIEM. No. 07. Bolognia, Italia.
17. Marcin Jasinki, Stanislaw Radkowski. Biespectrum as a Symptom of Damages in a Rolling Bearing Diagnostics. Scientific Research Comite.KBN No 9T12C04615.
18. A. C. McCormick, A. K. Nandi. (1999). Bispectral and Trispectral Feature for Machine Condition Diagnosis. IEEE Proceeding Visual Image Process. Vol. 146. pp. 229-234.
19. Jerry M. Mendel. (1991). Tutorial on Higher-Order Statistics (Spectra) in Signal Processing and System Theory: Theoretical Results and Some Applications. IEEE Vol. 79. No. 3. pp. 278-298.
20. A. Swami, J. Mendel, C. Nikias. (1998). Higher-Order Spectral Analysis Toolbox: For Use with MatLab. User's Guide Version 2. MathWorks.
21. Brillinger David, Rosenblatt Murray. (1967). Computation and Interpretation of k-The Order Spectra. From B. Harris: Spectral Analysis of Time Series.
22. SKF. Frequency calculator-Bearing frequencies calculation.
23. Zulma Medrano, Carlos Pérez; Julio Gómez, (2015)b. Diagnóstico de fallas en rodamientos en un generador síncrono: Nueva técnica de diagnóstico de falla en rodamientos en un generador síncrono a través de señales vibro-acústicas